Review

Advances in Sno2-Based Nanomaterials for Photocatalysis, Supercapacitors, and Antibacterial Activities

Naveen Chandra Joshi*[1], Rajesh Singh[1], Sanjay Upadhyay[1], Niraj Kumar[1], Anita Gehlot[1], and Chetana S[1], Chander Prakash[2*], Kuldeep K. Saxena[3], Dhanesh G. Mohan[4*], Jacek Tomków[5]

1 Division of Research & Innovation, Uttaranchal University Dehradun (India), drnaveen06joshi@gmail.com, drrajeshsingh004@gmail.com, bannudsanjay@gmail.com, nirajunisci2k@gmail.com, eranita5@gmail.com, chetana.s.mech@gmail.com
2 School of Mechanical Engineering, Lovely Professional University, Phagwara, Punjab- 144411, India, *: chander.mechengg@gmail.com
3 Department of Mechanical Engineering, GLA University, Mathura-281406, India, saxena0081@gmail.com
4 Department of Material Processing Engineering, Zhengzhou Research Institute, Harbin Institute of Technology, Zhengzhou, China, dgmohan@hit.edu.cn
5 Faculty of Mechanical Engineering and Ship Technology, Gdańsk University of Technology, Poland, jacek.tomkow@pg.edu.pl
*Correspondence: drnaveen06joshi@gmail.com; chander.mechengg@gmail.com; dgmohan@hit.edu.cn

Abstract: Tin (IV) oxide nanoparticles (SnO_2 NPs) have received a lot of interest because of their interesting features. SnO_2 NPs have proven productive in a range of fields, including water purification, supercapacitors, batteries, antibacterial and antioxidant agents, and others. SnO_2-based nanoparticles found a wide range of applications after incorporating materials with varying chemical compositions. SnO_2 NPs and their nanocomposites have been used effectively as antibacterial agents against various pathogenic bacteria, photocatalysts for dye degradation, and electrode materials for supercapacitors (SCs). This article covers the characteristics of SnO_2 NPs, SnO_2 nanocomposite materials, applications of SnO_2 NPs and their composite materials, including antibacterial, energy storage, and photocatalysis, as well as some significant recent studies.

Keywords: SnO_2 NPs and their nanocomposites; Photocatalysis; Supercapacitors; Antibacterial activities

1. Introduction

Nanomaterials are used in a wide range of industries, including storing energy, water treatment, nanomedicine, fuel cells, sensing, catalysis, optoelectronics, and tunable resonant devices. This is because nanoscaled materials have higher surface-to-volume ratios than their microsized counterparts, which results in unsaturated and thus more reactive surface atoms [1]. If a material has at least one dimension smaller than 100 nm, it is referred to as a nanoparticle. As opposed to bulk materials of the same substances, engineered nanoparticles possess unique features that are not present in them. The thermal, optical, electrical, and surface properties of metal and metal oxide nanoparticles differ from those of their original bulk components in a number of ways. They also show multiple physicochemical characteristics [2]. Gold (Au), copper (Cu), silver (Ag), manganese (Mn), platinum (Pt), palladium (Pd), magnesium oxide (MgO), titanium oxide (TiO_2), zinc oxide (ZnO), cupric oxide (CuO), calcium oxide (CaO), manganese oxide (MnO_2), tin oxide (SnO_2), and iron oxides include the most widely known metal-based nanoparticles [3-7]. Because of their improved features, these nanoparticles have been used in catalysis, water remediation, pharmaceuticals, the textile industry, and in other fields of contemporary science and engineering [8]. Tin (IV) oxide nanoparticles (SnO_2 NPs) have received a lot of interest because of their potential applications in research and industrial fields [7-

 doi:10.20944/preprints202211.0494.v1

10]. SnO_2 is a prominent n-type wide-bandgap semiconductor, and due to the variety of controllable physicochemical features of SnO_2-based nanostructures, they are emerging as one of the most significant classes. Many studies have recently reported the synthesis of SnO_2-based nanocomposite materials, which can significantly improve performance [8,11]. SnO_2 NPs and their nanocomposites have been successfully employed as the electrode materials of SCs, as photo-catalysts for dye degradation, and as antibacterial agents against different pathogenic bacteria [12-14]. Due to their high specific capacitance and chemical stability, SnO_2-based SCs have received a lot of attention [8]. The SnO_2-based nanomaterials have been predicted to be potent photocatalysts for the degradation of organic pollutants in wastewater due to extraordinary properties such as transparency, inertness, photosensitivity, environmental friendliness, and stability [15]. SnO_2 NPs have received interest as an antibacterial agent and have been considered significant in inhibiting the development of numerous bacterial strains. Other significant features of SnO_2 NPs include antitumor, antioxidant, and anticancer activities [16]. In this article, we have discussed the properties of SnO_2 NPs, nanocomposite materials of SnO_2, applications (especially antimicrobial, energy storage, and photocatalysis) of SnO_2 NPs and their composite materials, and some important current studies.

2. SnO_2 nanoparticles (SnO_2 NPs) and SnO_2-based nanocomposites

SnO_2, an n-type wide-bandgap semiconductor, and point defects act as donors or acceptors, which causes it to conduct electricity. Tetragonal rutile structures result from SnO_2 crystallisation. Six oxygen atoms surround each tin atom, whereas three tin atoms surround each oxygen atom. This material's numerous distinctive qualities make it extremely valuable in a wide variety of applications [17]. Adjusting the SnO_2 conduction band minimum and, in turn, altering its optical absorption characteristics has received a lot of scientific attention [10]. The printed electronics application (electron transport and hole blocking layers) is provided by the specific electronic properties of SnO_2 NPs. Additionally, they may carry out electron injection and charge recombination activities for a variety of thin film designs, such as organic light-emitting diodes, printed photodetectors, and organic photovoltaics [10,17]. SnO_2 possesses high electrical conductivity, high optical transparency, low electrical resistance, and stability under a variety of environmental conditions. It is being thoroughly investigated because of its potentially catalytic uses [18]. The important properties of SnO_2 NPs are depicted in figure 1. SnO_2 NPs have attracted a great deal of attention because of their prospective uses in sensors, SCs, lithium-ion batteries, catalysis, field emission displays, light-emitting diodes, optoelectronics, medicine, photocatalysis, and antistatic coatings [7–10]. (Fig. 2). Heterogeneous or hybrid materials contain at least one component made up of nanoscaled particles known as nanocomposites. The components, structure, and interfacial interactions of each specific property have a significant impact on them. In addition to improved economic potential for a number of industrial sectors that are highly beneficial to humanity and the environment [19,20]. Metal doped SnO_2, conducting polymers/SnO_2, transition metal oxides (TMOs)/SnO_2, graphene/SnO_2, and other important SnO_2 based nanocomposites have been used in solar cells, SCs, Li-ion batteries, water purification, catalysis, sensors, medicine, electronics devices, and other sectors. The increased effectiveness of its practical applications may be due to the improved properties, such as increased surface area, chemical and thermal stability, increased surface activities or number of active surface sites, enhanced charge transfer processes, mechanical strength, reduced electron-hole recombination, etc. [21-30].

Preprints (www.preprints.org) | NOT PEER-REVIEWED | Posted: 28 November 2022 doi:10.20944/preprints202211.0494.v1

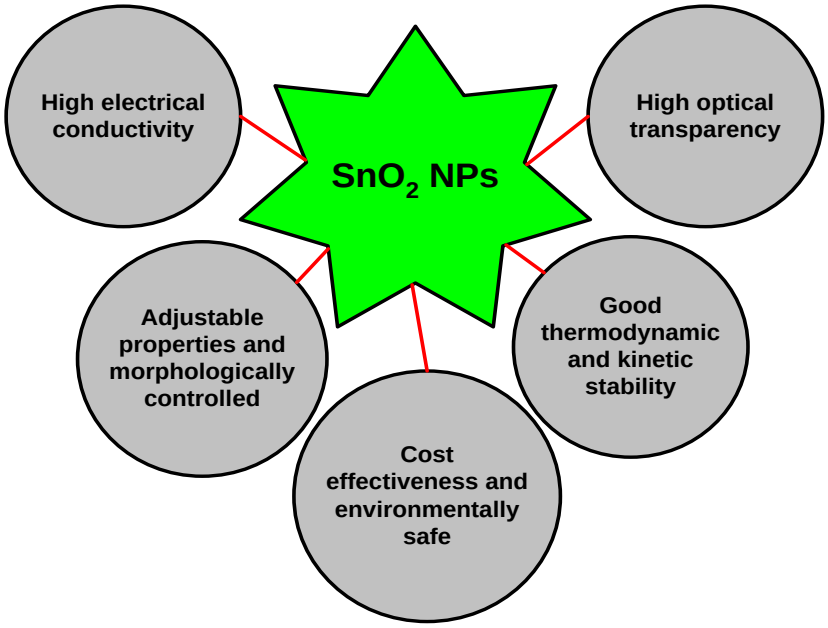

Figure 1: Some important features of SnO_2 NPs

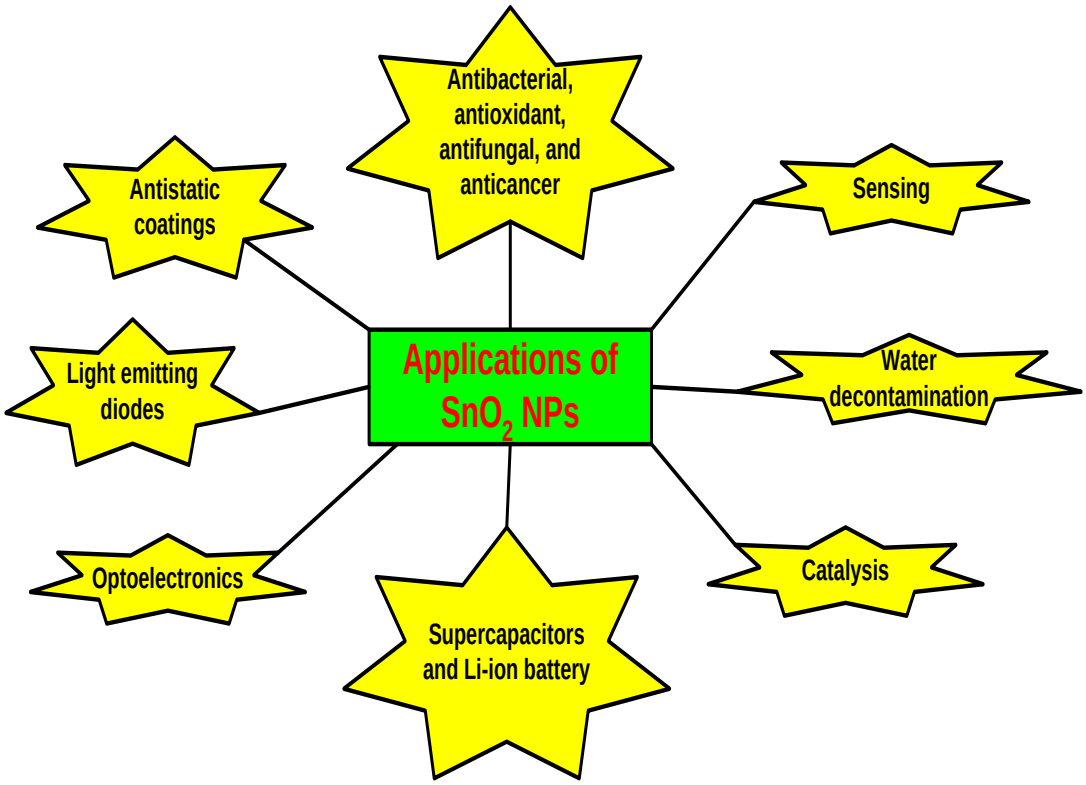

Figure 2: Applications of SnO_2 NPs

3. Photo-catalytic activity of SnO_2 NPs and its nanocomposites

Various techniques are used in the treatment of wastewater that has become contaminated by dye, as it is a major global concern. Among the treatment methods for wastewater containing dyes is photocatalysis [31]. The dyes are subsequently released

 doi:10.20944/preprints202211.0494.v1

into both fresh and saltwater after being used in the leather, plastic, pharmaceutical, paper, food, and textile industries. The dyes are water-soluble organic species, and both the dyes directly and their derivatives are dangerous to humans and other living organisms [32]. There is a broad range of synthetic dyes found in wastewater that have been used in industry and are typically referred to as azo, sulphur, indigo, anthraquinone, triphenylmethyl (trityl), and phthalocyanine derivatives [33]. They are very difficult to remove from water and wastewater because of their high solubility. Most dyes irritate the skin, induce headaches, harm the eyes, cause coughing and nausea, skin discoloration, suppress the immune system, and cause other health issues [34,35]. Metal oxide based photocatalysts show charge transport properties, adequate electronic structure, and ability to adsorb suitable radiation. The desired band gap, large surface area, stability, appropriate morphology, and reusability are the important aspects of the photocatalytic system [32,35]. When the photocatalyst is subjected to incident photons, electrons are shifted to the conduction band (CB), while holes formation takes place in the valence band (VB). The photogenerated pair (e^-/h^+) has the ability to reduce or oxidise a pollutant that has been adsorbed on the surface of catalyst. Metal-based catalysts have two ways to show photocatalytic behaviour; one, the oxidation of OH^- ions to form OH* radicals, and second, the reduction of oxygen to produce O_2 radicals. Organic pollutants can be broken down or converted into less hazardous by-products by radicals and anions [35,36]. Figure 3 depicts the mechanism of photocatalytic process. The overall photocatalytic process is affected by different operational parameters such as dye concentration, irradiation time, morphology of catalysts, dosage of photocatalyst, reaction temperature, pH of dye containing solution, and light intensity [34] (Fig. 4). In general, as dye concentration increases and catalyst quantities remain constant, the percentage of degradation decreases. It may be because of the availability of a limited number of active sites on catalysts [37]. Hole-electron pair separation suffers with recombination at lower light intensities, which lowers the generation of free radicals and, as a result, decreases the rate of degradation of organic components, which could be eliminated at higher light intensities [38]. It was found that when the catalyst concentration increased, the rate at which the dye degraded also increased. Because there are more active sites available, dye molecules can interact with them more readily [39]. The rate of dye degradation typically increases with irradiation time, but after a time it remains stable because the catalyst surface is saturated with dye molecules [40]. When the pH is increased beyond the nanophotocatalyst's isoelectric point, the photocatalyst surface becomes negatively charged. The functional groups are protonated as the pH lowers, which enhances the positive charge on the surface of the photocatalyst. When the pH is higher, the negatively charged surfaces on photocatalyst enhance the uptake of cationic molecules, whereas when the pH is lower, it favours uptake of anionic molecules [41]. Other crucial factors are surface morphology and particle size. The number of photons striking the catalyst determines the rate of reaction, indicating that the reaction occurs solely in the received phases of the photocatalyst [42]. The reaction temperature enhances the rate of photocatalytic activity. The optimum temperature for the effective photomineralization of organic substances has been noted to be in the range of 20 to 80 °C [41].

Preprints (www.preprints.org) | NOT PEER-REVIEWED | Posted: 28 November 2022 doi:10.20944/preprints202211.0494.v1

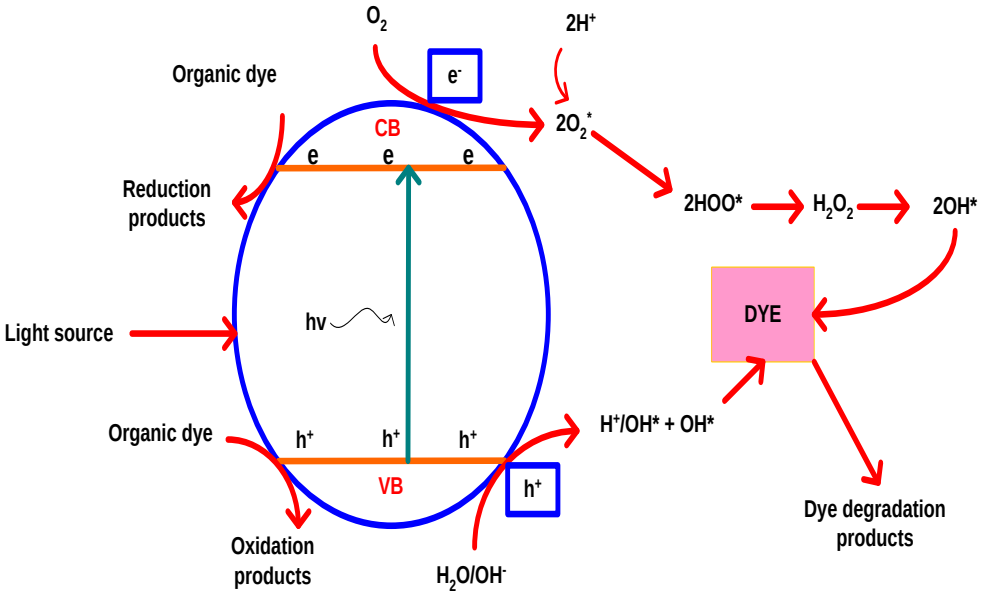

Figure 3: General mechanism of photocatalysis

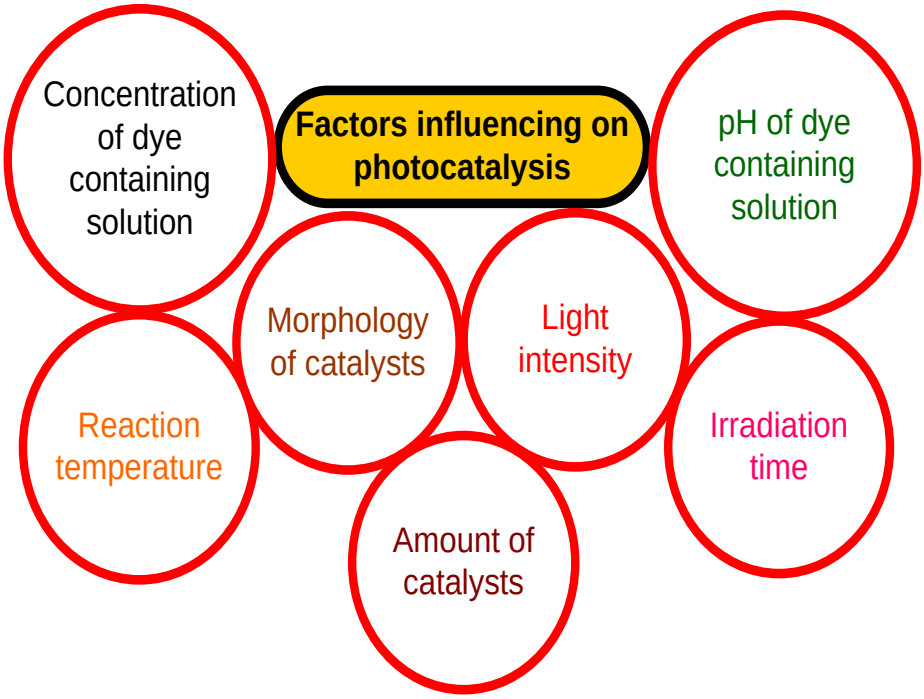

Figure 4: Factors influencing on photocatalysis

Preprints (www.preprints.org) | NOT PEER-REVIEWED | Posted: 28 November 2022 doi:10.20944/preprints202211.0494.v1

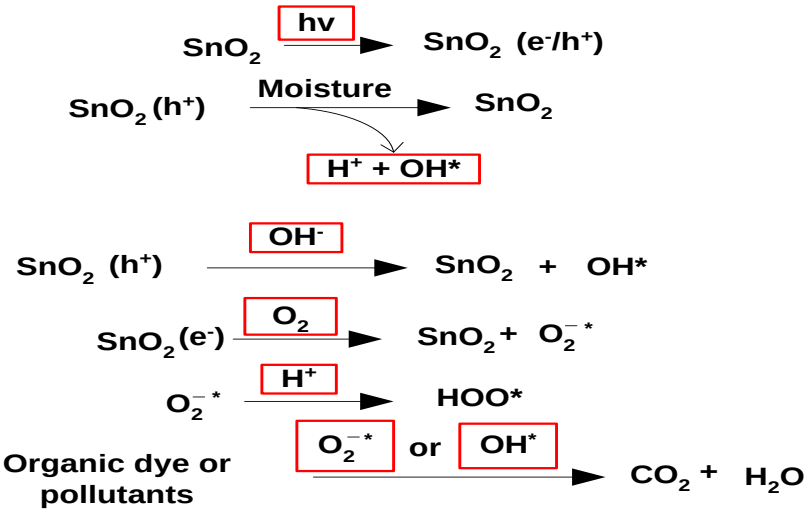

Figure 5: Photocatalytic mechanism of SnO_2 NPs

Tin-oxide (SnO_2) nanoparticles have been predicted to be potent photocatalysts for the degradation of organic pollutants in aqueous media based on their advanced characteristics, which include low cost, chemical and biological inertness, non-toxicity, ease of fabrication, and light sensitivity [15]. SnO_2 is analogous to titanium dioxide (TiO_2), a prominent photocatalyst, in aspects of band gap, morphology, and chemical resistance. SnO_2 is also poorly absorbed by the human body and has no negative impact on health. High photocatalytic activity is expected for SnO_2 based materials [13]. A heterojunction is formed between two different semiconductors with different band structures. As a consequence, addressing the problems with a single SnO_2-based photocatalyst can be achieved through creating a heterojunction with SnO_2 [11]. Figure 5 depicts the possible mechanism of photocatalysis by SnO_2 NPs. Conventional heterojunctions are categorised into type-I (straddling gap), type-II (staggered gap), and type-III (broken gap) [43] (Fig. 6). The h^+s and e^-s are shifted from first semiconductor (SC-I) to second semiconductor (SC-II) in the same direction in type I heterojunction. In a type II heterojunction, the h^+ and e- ions shift in the opposite direction [38]. Because there are fewer opportunities for charge transfer between the different semiconductors in type III heterojunctions compared to the other types. A redox reaction occurs on different semiconductor surfaces, and the h^+ ions of SC-I recombine with the photoexcited e- ions of SC-II [44]. The type-II heterojunction is the effective conventional heterojunction because of spatial separation of electron-hole pairs among the aforementioned conventional heterojunctions [43,44] (Fig. 6).

Preprints (www.preprints.org) | NOT PEER-REVIEWED | Posted: 28 November 2022 doi:10.20944/preprints202211.0494.v1

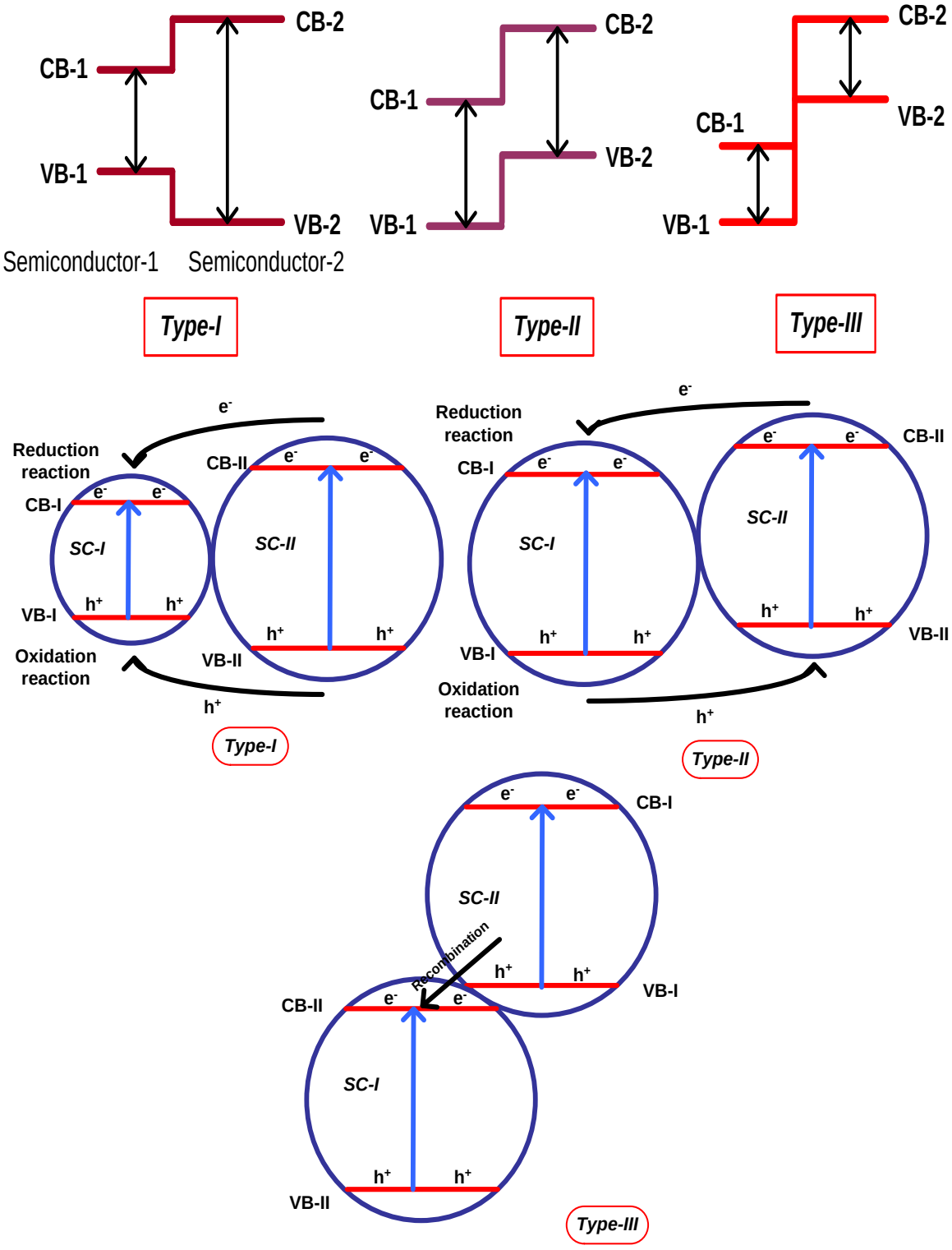

Figure 6: Type of heterojunctions

The precipitation approach was studied by Kim et al. [13] for the fabrication of SnO_2 NPs. Applying X-ray diffraction (XRD), transmission electron microscopy (TEM), and X-ray absorption spectroscopy (XAS), the synthesised SnO_2 NPs were characterized. The agglomerated nanoparticles can degrade methylene blue (MB) 3.8 times faster than bulk SnO_2 and have a

 doi:10.20944/preprints202211.0494.v1

particle size of 4 to 5 nm. The photocatalytic activity of hydrothermally produced SnO_2 NPs for the degradation of eosin red (ER), MB, and rhodamine B (RhB) was reported by Xing et al. [45]. SnO_2 NPs are still highly photocatalytically active after five cycles. RhB, ER, and MB all degraded at rates of 98%, 91%, and 53%, respectively. The catalytic activity of SnO_2 NPs against the degradation of MB and CR was investigated by Paramarta et al. [15]. The results indicate that SnO_2 NPs have a well-crystalline structure with crystallites that are 44 nm in size. By monitoring the decrease in dye concentration before and after exposure to ultrasonic and light radiation, respectively, it has been possible to determine the degradation of organic dyes. Other factors, including pH, catalyst dosage, and scavenger dosage, have also been studied for their effects. To confirm the stability of the utilised catalysts, experiments on reusability have also been performed. Yuan and co-workers [46] investigated the photodegradation of methyl orange (MO) using SnO_2 NPs under different batch conditions. The particle size of SnO_2 NPs was found to be 30 to 40 nm. These nanoparticles were capable of degrading 97 % of dye after 120 min. He and Zhou [47] have reported the photocatalytic ability of sphere-line SnO_2 NPs for the degradation of RhB under UV-light illumination. The SnO_2 spheres' surfaces will become rough as the reaction time increases and smooth as the time goes on. Tammina et al. [48] studied the effect of the size of SnO_2 NPs on the degradation of MB. They observed the maximum degradation takes place due to the smaller size of SnO_2 NPs. The water decolourisation was completed within 20 min of contact time. Pouretedal and other [49] workers reported the synthesis of SnO_2 NPs using controlled precipitation method and its photocatalytic behaviour. The SnO_2 NPs have been characterised by the help of XRD, TEM, UV-Vis, and other methods. At 150 minutes, SnO_2 NPs degrades MB was more than >95% at a basic pH of 11.

The green fabrication of SnO_2 NPs with the leaf extract of *Delonix elata* was taken into account by Suresh et al. [50]. SnO_2 NPs were synthesised using the microwave, wet chemical, and sonication processes. RhB was broken down by the greenly synthesised SnO_2 NPs under UV light. After 150 minutes of radiation exposure, 92.8% of RhB had degraded. Karthik et al. [51] studied the synthesis of SnO_2 NPs using the *Andrographis paniculate* extract. With a particle size of 27 nm, the tetragonal structure of SnO_2 NPs has been found. The photodegradation of CR dye under sunlight used the biologically synthesised SnO_2 NPs. The experimental results showed that the bioinspired SnO_2 NPs were found to be very effective for degrading CR dye. Wicaksono et al. [52] studied the use of *Amaranthus tricolor* extract in the synthesis of SnO_2 NPs. The photocatalytic behaviour of SnO_2 NPs has been assessed in the photodegradation of bromophenol blue (BPB) using photocatalytic and photooxidation methods in the presence of H_2O_2. Physical-chemical analyses have validated the photoactive properties of SnO_2 NPs. Both of the routes for degradation follow pseudo-second order kinetics, and the degradation was observed from the altered spectra of the treated solution. Pomegranate (*Punica granatum*) leaves were used by Singh et al. [53] to synthesise SnO_2 NPs in an inexpensive and environmentally friendly manner. In this study, SnO_2 NPs that had been successfully synthesised with a particle size of 20 nm were employed as an effective photocatalyst to degrade MB dye in the presence of sunlight. At 240 min, 91.5% of the degradation efficiency was estimated. The degradation of MB under UV light was carried out by Viet et al. [54] using hydrothermally synthesised SnO_2 NPs. The 3 nm-sized, highly photocatalytically active nanoparticles were synthesised; 88.8% of the

 doi:10.20944/preprints202211.0494.v1

MB solution was degraded by SnO_2 NPs after 30 minutes of UV light, and 90.0% after 120 minutes of UV irradiation. *Pometia pinnata* leaf extract was used by Fatimah et al. [55] to biofabricate flower like SnO_2 NPs. On the photooxidation of bromophenol blue (BPB), the nanoparticles' photocatalytic activity was investigated. The diameter of the nanoparticles, which ranged from 8 to 20 nm, was seen to be uniformly spherical. The SnO_2 NPs exhibited great photocatalytic activity in the photooxidation of BPB as the degradation efficiency exceeded 99.9%, and the photocatalyst displayed reusability as the degradation efficiency values were little modified until the fifth cycle. The treatment of wastewater containing dye has attracted a lot of interest using SnO_2-based nanocomposites as photocatalysts; hazardous dyes are degraded with remarkable efficiency (Table 1) [56-68].

Table 1: SnO_2-based nanocatalysts for dye degradation

SnO_2-based nanocatalysts	**Degraded dye**	**Maximum degradation (%)**	**References**
SnO_2/rGO	MB	98.2	[56]
Bi/SnO_2/TiO_2-graphene	Pentachlorophenol (PCP)	84.0	[57]
SnO_2/TiO_2/RGO	RhB	83.8	[58]
ZnO/SnO_2–Sn	MB	95.6	[59]
SnSe/SnO_2	RhB	90.0	[60]
Fe_3O_4/SnO_2	Crystal violet	83.0	[61]
SnO/SnO_2	MB	64.5	[62]
ZnO/SnO_2	Biebrich scarlet (BS)	97.0	[63]
PbS/SnO_2	MO	87.0	[64]
B_4C/SnO_2	MB	79.4	[65]
SnO_2/CuO	MB	92.0	[66]
SnO_2/NiO	RhB	82.0	[67]
mpg-C_3N_4/SnO_2	RhB	93.0	[68]

4. SnO_2 NPs and its nanocomposites as electrode materials for SCs

Concerns about the consumption and production of electricity have been highlighted as a result of the energy crisis and the growing world population. Therefore, a more potentially powerful system for energy storage than what is available now is required [69]. Energy storage devices serve as a reservoir for the electrical system, accumulating excess energy generated during periods of high production and releasing it when needed [70]. SCs are energy-storage electrochemical systems with high energy and power densities, excellent charge-discharge rates, and an extra life span. These features contribute to high-energy storage capacity. This is necessary

Preprints (www.preprints.org) | NOT PEER-REVIEWED | Posted: 28 November 2022 doi:10.20944/preprints202211.0494.v1

for the advancement of technology. SCs have a high storage capacity, are bigger than normal capacitors, and have a low internal resistance. It bridges the gap between rechargeable batteries and regular capacitors [69,70]. Two parallel electrodes which are separated from each other by a separator constitute SCs. A separator is a conducting material coated with an electrolyte; when the voltage is applied, electrolyte ions adhere to the electrode's surface. Electrostatic double layer (EDL) formation is caused by charge build-up and interaction with the electrode surface. The EDL generation mechanism produces efficient charge-discharge cycles and is reversible. SCs experience substantial power as a consequence (Fig. 7) [71-73].

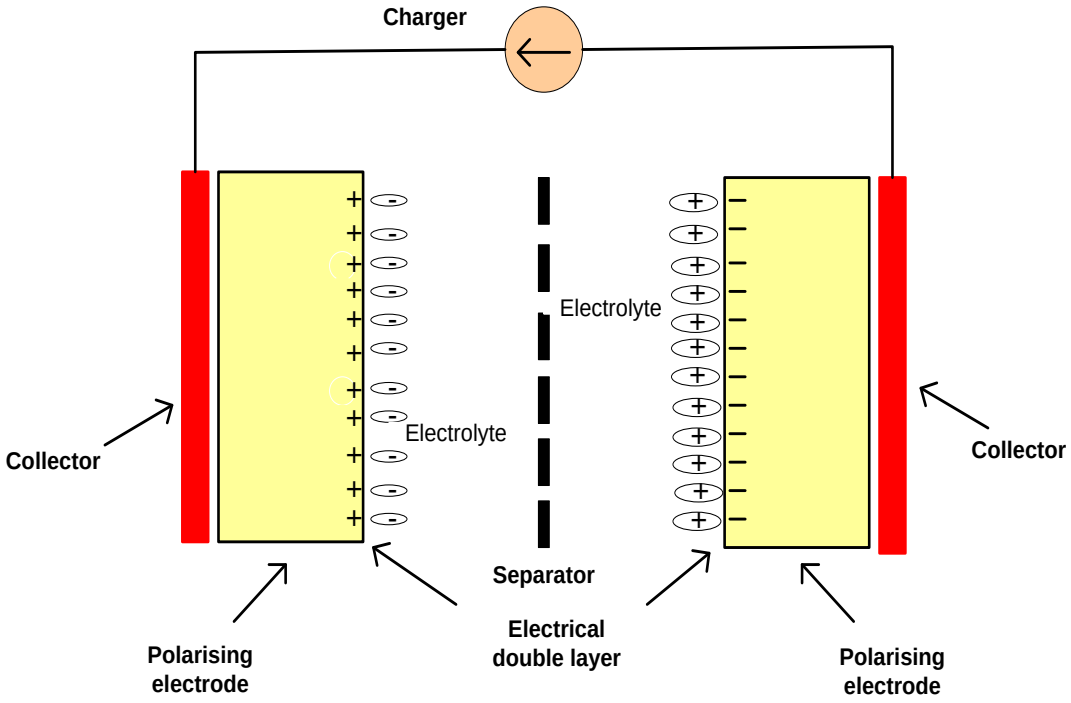

Figure 7: Supercapacitors (SCs)

SCs are divided into electrostatic double-layer capacitors (EDLC), pseudo-capacitors, and hybrid capacitors (Fig.8). The EDLC is made up of two electrodes, an electrolyte, and a separator. An electrolyte consists of cations and anions, and a separator is used to keep the two electrodes apart. In general, EDLC has electrodes of carbon and its derivatives, which have a significantly greater electrostatic double-layer capacitance [74-76]. Pseudo capacitors generally utilise metal oxide or conducting polymer-based electrodes. By transferring electron charges between an electrode and an electrolyte, these components store electrical energy. The transfer of electrons is a process of reduction-oxidation, or redox process. The hybrid capacitors are made up of double-layer capacitors and pseudo-capacitors [77-79]. Conducting polymers, carbon materials, and metal oxides have been employed as electrode materials in these SCs. The capability of one electrode to display electrostatic capacitance and the capability of the second electrode to show electrochemical capacitance. Hybrid SCs, which include an EDLC and a pseudocapacitor, act as capacitance enhancers due to their asymmetric behaviour [80].

Preprints (www.preprints.org) | NOT PEER-REVIEWED | Posted: 28 November 2022 doi:10.20944/preprints202211.0494.v1

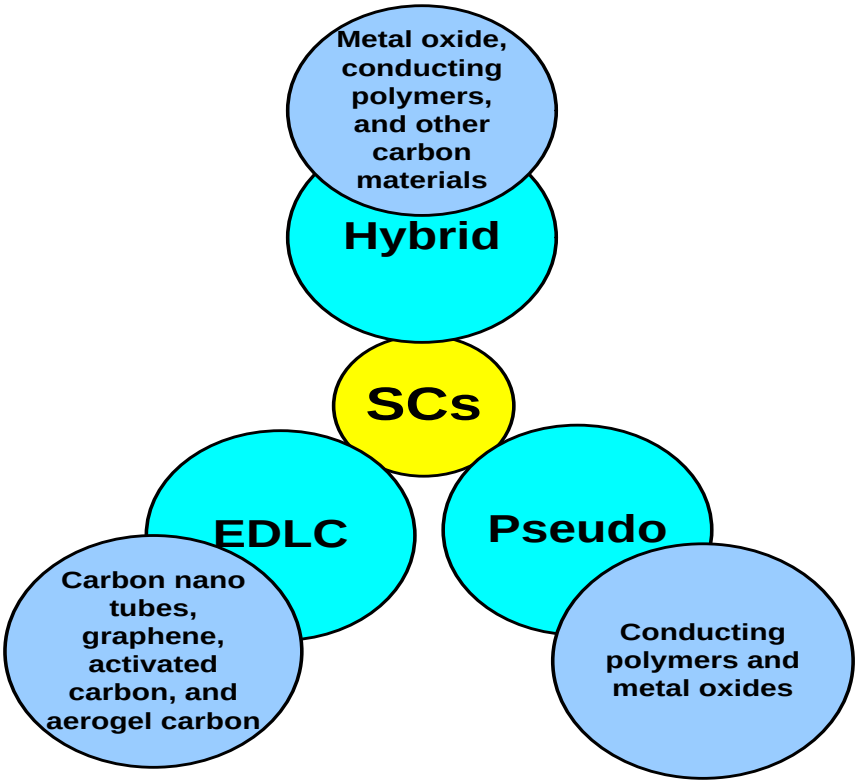

Figure 8: Classification of SCs

SnO_2 NPs are regarded as potent electrode material like RuO_2, Co_3O_4, and NiO, because of excellent physical and chemical properties, ease of synthesis, and cost-effectiveness [81]. Velmurugan et al. [82] studied on the SnO_2/graphene nanocomposite for SCs applications. The SnO_2/graphene composite was analysed using Fourier transform infra-red (FTIR), X-ray diffraction (XRD), and high-resolution transmission electron microscopy (HRTEM) methods. At a scan rate of 5 mV/s, a maximum specific capacitance of 818.6 F/g for the SnO_2/graphene composite was reported, confirming that the addition of graphene matrix significantly improved the electrochemical performances of SnO_2. The SnO_2/PPY/graphene-based electrode material for the SCs applications was reported by Wang et al. [83]. At 1 mV/s, it was found that this ternary mixture had a specific capacitance of 616 F/g. After 1000 galvanostatic cycles, the electrode exhibits improved cycle durability and no apparent deterioration. It has a specific power density of 9973.2 W/kg and an energy density of 19.4 Wh/kg. Ramesh et al. [84] investigated the SnO_2/NGO-based composite as an electrode material for SCs. SnO_2/NGO composite that has been examined utilising a variety of methods, including XRD, HR-TEM, SEM, and others. Some of the electrochemical properties of SnO_2/NGO included a specific capacitance of 378 F/g at a current density of 4 A/g and improved cycle stability up to 5000 cycles. Manikandan et al. [81] synthesised SnO_2 NPs by the coprecipitation process, and galvanostatic charge-discharge and cyclic voltammetry were used to assess the supercapacitor's electrochemical performance. A specific capacitance of 122 F/g was attained with a scan rate of 2 mV/s. The Zn_2SnO_4/SnO_2/CNT nanocomposite has been reported by Samuel and others [85] as a supercapacitor electrode. Cyclic voltammetry showed the enhanced electrode's capacitive performance with a specific capacitance of 260 F/g at a current density of 10 A/g. After 15000 galvanostatic charge/discharge cycles, the specific capacitance was retained with great precision (93%). The MnO_2/SnO_2 composite was developed by Feng et al. [86] and employed as an electrode for SCs. The composite provided 541.6 F/g capacitance at 1 A/g and has good cyclic stability. The specific capacitance of MnO_2/SnO_2 continues to remain at 498 F/g even after 1500 cycles of testing at 2 A/g. The electrochemical performance of SnO_2/r-GO composites was reported by Zhang et al. [87]. According to the results, the composite's specific capacitance may achieve 262.2 F/g at a current density of 100

 doi:10.20944/preprints202211.0494.v1

mA/g. The composite retains its original capacitance of 96.1% after 6000 cycles, demonstrating remarkable electrochemical performance. Liu et al. [88] studied the electrochemical behaviour of SnO_2-based composites, such as SnO_2/NiO, SnO_2/Co_3O_4, and SnO_2/MnO_2. Maximum specific capacitance, strong rate capability, and outstanding cycling stability were all exhibited by the SnO_2/MnO_2 electrode. In table 2, other SnO_2 based electrode materials for SCs are listed.

Table 2: SnO_2-based electrode materials for SCs

SnO_2-based electrode materials	**Specific capacitance**	**Energy and power density**	**Cyclic stability**	**References**
CuO/SnO_2	1972 F/g at 1 A/g	117.32 Wh/ kg at 13 624.2 W/kg	96.05% after 10 000 cycles	[89]
SnO_2/NiO	464.67 F/g at 5 mV/s	-	84.4% after 1,000 cycles	[90]
CC/ZnO/MnO_2	585.8 F/g at 1.0 Ma/cm^2	-	100 % after 10,000 cycles	[91]
Fe_2O_3/SnO_2	562.3 F/g at 1 A/g	50.2 Wh/kg at 650 W/kg	92.8 % after 3000 cycles	[91]
Zn_2SnO_4/SnO_2/CNT	260 F/g at 10 A/g	98 Wh/kg at 1000 W/kg	93 % after 15000 cycles	[85]
r-SnO_2/GN	947.4 F/g at 2 mA/cm^2	-	88.2 % after 1000 cycles	[92]
Co_3O_4/SnO_2/MnO_2	225 F/g at 0.5 A/ g	-	90.7% after 6000 cycles	[93]
MnO_2/SnO_2	800 F/g at 1 A/g	35.4 W h/kg at 25 kW/kg	98 % after 2000 cycles	[94]
CNTs/SnO_2	113.6 F/g at 2 A/g	20.3 Wh/kg at 118W/kg	92 % after 1000 cycles	[95]
MnO_2/SnO_2	367.5 F/g at 50 mV/s	-	91.3% after 2000 cycles	[96]

5. Antimicrobial activity of SnO_2 NPs/ SnO_2 based nanocomposites

The antibacterial properties of metal and metal oxide engineered nanoparticles have attracted extensive interest over the last twenty years [97]. The need for new antibiotic agents has been emphasised by the continuous rise of bacterial resistance. Metal-based NPs, which have shown potent antibacterial action in a vast majority of investigations, are some of the most promising of these novel antibiotic agents [98]. MONPs are shown to be an efficient bacterial strain inhibitor [99]. It is essential to actively explore nanomaterials at the nanoscale since the antibacterial activity of NPs depends on their size and form. Various metal oxides with varying shapes and sizes have recently been the subject of basic and applied research for their possible use in a wide range of applications, including sensing, energy storage, antibacterial agents, semiconduc-

 doi:10.20944/preprints202211.0494.v1

tors, etc. Metal-based nanoparticles with antibacterial properties have been found to include silver (Ag), gold (Au), copper oxide (CuO), calcium oxide (CaO), zinc oxide (ZnO), magnesium oxide (MgO), tin oxide (SnO_2), silver oxide (Ag_2O), and titanium dioxide (TiO_2) [1,2,99-102].
The MONPs have been used in the destruction of gram-positive and gram-negative bacteria, and other pathogens. In addition to these advantages, SnO_2 has drawn attention for its effectiveness as an antibacterial agent in preventing the growth of several bacterial strains. Other significant biological features such as antioxidant, anticancer, and antitumor activities of SnO_2 NPs have also been found [1,2]. Formation of ROS (Reactive oxygen species), damage of cell wall/membrane, metal-ion release, and particle internalisation into bacteria are some of the unique mechanisms that have been proposed for these substances' antibacterial effects, though their exact mechanism is still up for debate (Fig. 9). Metal oxides easily undergo redox reactions that are promoted by light. Their unique electrical configuration, which includes features like an occupied CB and an empty valence band VB, is the main reason for this activity. The generated electrons and holes have a probability of interacting with other species like O_2 and H_2O adsorbed on the metal oxide surfaces. The ROS ($OH\bullet$), hydrogen peroxide (H_2O_2), and superoxide ($O_2^{-}*$) considered to degrade the bacterial cell into CO_2, H_2O, and other nontoxic substances by several chain redox processes [103,104] (Fig. 10). The first phase of the antibacterial mechanism is the interaction of the nanoparticles with the cell membrane. The cell membrane's structural modifications and inhibition of its transport channels proceed subsequently. After this, NPs may be incorporated, causing ionisation inside the cell and the destruction of intracellular structures, ultimately resulting in cell death [105]. The other major mechanistic ways in which NPs exhibit antibacterial behaviour are the deactivation of enzymes, their attachment to NPs, and the disruption of the hydrogen bonding between two antiparallel strands of DNA [101].

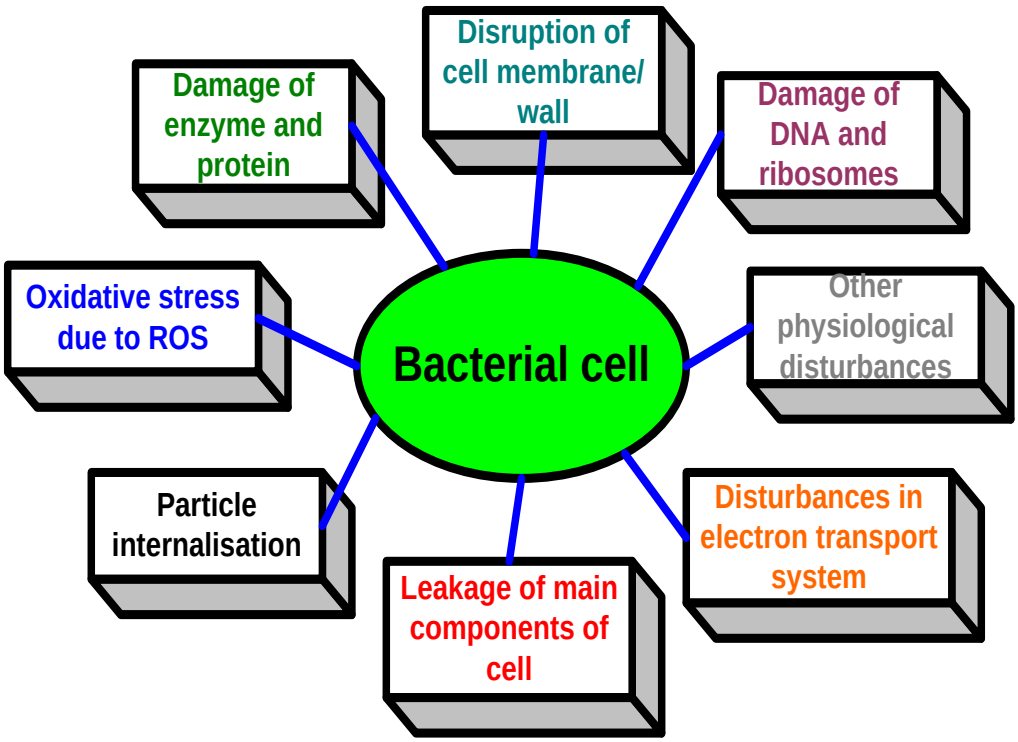

Figure 9: Some basic ways to understand the antibacterial activity of MONPs

Preprints (www.preprints.org) | NOT PEER-REVIEWED | Posted: 28 November 2022 doi:10.20944/preprints202211.0494.v1

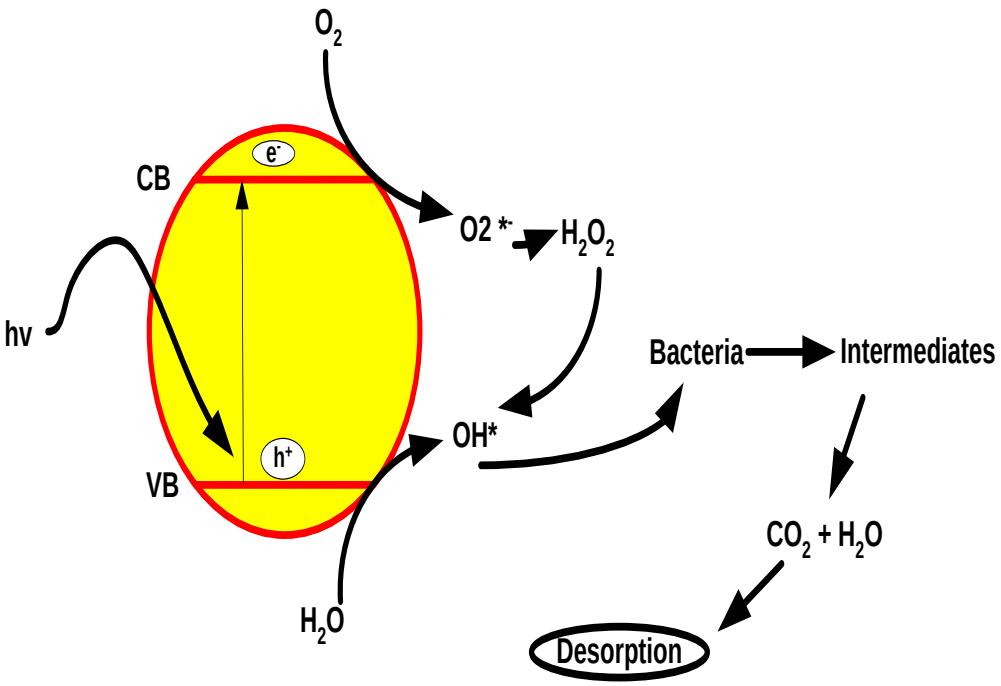

Figure 10: Destruction of bacterial cell due to formation of ROS

Pometia pinnata leaf extract was used by Fatimah et al. [55] for the biofabrication of flowers like SnO_2 NPs. Antibacterial testing revealed that the synthesised SnO_2 NPs exhibit an inhibition of the tested bacteria and have the potential to be used in other medicinal applications. The SnO_2 NPs have strong antibacterial activity against both the gram-negative and gram-positive bacteria that were used in testing, suggesting that they might be further improved for use in biomedical applications. Amininezhad et al. [14] studied the synthesis of SnO_2 NPs using a solvothermal process. The *Escherichia coli* (*E. coli*), and *Staphylococcus aureus* (*S. aureus*) were rendered inactive by the SnO_2 NPs. It was observed that SnO_2 NPs exhibit significantly more activity against *E. coli* than *S. aureus*. The shape of the cellular membrane and the resistivity of the outer membrane to the reactive oxygen species formed at the photocatalyst surface also influence the rate of photoinactivation of bacteria in addition to cell wall thickness.

A microwave irradiation approach was used by Apsana et al. [106] to synthesise SnO_2 NPs, which were then examined for their antibacterial activity. *Proteus vulgaris* (*P. vulgaris*), *E. coli*, *Pseudomonas aeruginosa* (*P. aeruginosa*), *Klebsiella pneumonia* (*K. pneumonia*), and *Morganella morganii* (*M. morganii*) were treated with SnO_2 NPs. Due to the SnO_2 NPs' smaller size and the crucial phenolic chemicals in *Ocium sanctum* leaves, remarkable antibacterial activity has been seen in *O. sanctum* extract-derived SnO_2 NPs. The synthesis of SnO_2 NPs using *Alovera* extract was reported by Ayeshamariam et al. [107]. They found that SnO_2 NPs had more potent anti-bacterial and anti-fungal capabilities than bulk SnO_2, especially for *Streptococcus pyogenes*, *Aspergillus niger* and *Mucor indicus* pathogens. SnO_2 NPs were synthesised by Khanom et al. [108] for the inactivation of *S. aureus* and *E. coli*. Antibacterial activity diminishes as the amount of nanoparticles in the solution decreases. SnO_2 NPs have nearly the same susceptibility to the gentamycin antibiotic, and *E. coli* exhibits no resistance to nalidixic acid. When used against *S. aureus*, SnO_2 NPs are found to be more sensitive than the both antibiotics.

Kamraj et al. [109] studied the antibacterial activity of SnO_2 NPs against *E. coli* and *S. aureus* bacteria. They have seen that SnO_2 NPs showed more antibacterial activity against *E. coli* than *S. aureus*. Because *E. coli* lacks a cell wall, nanoparticles could easily penetrate, producing greater cell damage than in *S. aureus*. Gowri et al. [110] also reported the antimicrobial activity of SnO_2 NPs against *E. coli* and *S. aureus*. They found that SnO_2 NPs show good antibacterial activity.

 doi:10.20944/preprints202211.0494.v1

Additionally, they observed maximum inhibition of *S. aureus* strain as compared to *E. coli*. Fatimah and co-workers [111] reported biofabricating SnO_2 NPs with the intervention of *Pometia pinnata* leaf extract. The bacterial strain such as *K. pneumonia*, *E. coli* and *S. aureus*, and *Streptococcus pyogenes* (*S. pyogenes*) were used to evaluate the antibacterial activity. The findings of the antibacterial test showed that the synthesised SnO_2 NPs inhibit the examined bacteria and have the potential to be used in other medicinal applications. Din et al. [112] used *Populus ciliate* leaf extract to synthesise SnO_2 NPs, which were then examined using several physico-chemical methods. The antibacterial properties of SnO_2 NPs were examined against *S. aureus*, *S. pyogenes* and *K. pneumonia*, and *E. coli*. With increasing nanoparticle concentration, it was shown that both antioxidant and antibacterial activities increased. Table 2 lists other SnO_2-based materials for antibacterial activity against different bacteria.

Table 3: SnO_2-based nanomaterials as antimicrobial agents

SnO_2-based materials	**Bacterial species**	**Zones of inhibition (mm or %)**	**References**
Ag-doped SnO_2	*S. aureus*, *E. coli*, *K. pneumoniae*, *P. aeruginosa*, *E. faecali*, and *B. cereus*	27 mm, 25 mm, 26 mm, 22 mm, 27 mm, and 23 mm	[113]
Cu/SnO_2	*S. aureus* and *P. aeruginosa*	10 mm and 12 mm	[114]
ZnO/SnO_2	*S. aureus*, *L. monocytogenes*, *E. coli*, and *S. typhi*	100%, 90%, 100%, and 80 %	[115]
Co-doped SnO_2	*E. coli* and *B. subtilis*	16 and 22 mm	[116]
Zr/SnO_2	*E. coli* and *S. aureus*	7 and 5 mm	[117]
Fe/SnO_2	*E. coli*	80%	[118]
Au/SnO_2	*B. subtilis* and *E. coli*	30 and 16 mm	[119]
S-GO-SnO_2	*E. coli* and *P. gramin*	>50%	[30]
Ni-doped SnO_2	*E. coli*	60%	[120]
Al-Bi/SnO_2	*S. aureus* and *B. cereus*	34 and 41 mm	[121]

6. Some important current studies:

Inorganic metal-based nanoparticles are regarded as one of the most promising materials for a variety of scientific and industrial uses. Because of their superior features, ease availability, and low cost, SnO_2 NPs have attracted a lot of interest. The SnO_2 and SnO_2 based materials have been used by different researchers in photocatalysis, SCs, and antibacterial activity as of the present (year 2022). Xiao et al. [122] investigated the photocatalytic degradation of RhB using F-doped SnO_2. The RhB degraded at a rate of 92.9% in 25 min following a 5-hour solvent heat treatment with polyethylene glycol (PEG) surfactant and F-doped SnO_2. Nazim et al. [123] have synthesised SnO_2 NPs functionalized with gallic acid (SnO_2/GA). Under ideal circumstances, the SnO_2/GA was able to degrade citalopram by 88.4% in 1 hour under UV light. The pseudo-first order rate of citalopram degradation was tracked. Water samples taken after several cleaning

 doi:10.20944/preprints202211.0494.v1

validation cycles of the citalopram manufacturing lines were effectively treated using the improved technique. The SnO_2/GA was examined for 3 cycles of reuse without noticeably losing activity. ZnO-SnO_2 nanoparticles were used by Dugosz et al. [124] for the photodegradation of dye mixtures. For the degradation of MB, RB, TB, MO, and YQ, respectively, the dye removal efficiencies after 60 min were 76.4, 72.6, 62.4, 77.0, and 92.4%. When the photodegradation efficiencies of ZnO-SnO_2 were evaluated with binary and ternary dye mixes, they were comparable to those of the single mixtures, suggesting that this material may eventually be employed in commercial applications. Gao et al. [125] demonstrated a photocatalytic CO_2 reduction. In this study, a unique defect engineering method was developed to produce $Sn_xNb_{1}xO_2$ by a sustainable hydrothermal method that significantly substitutes Nb into SnO_2. When compared to a pure SnO_2 sample, the $Sn_xNb_{1}xO_2$ solid solution sample performed much better in terms of photocatalytic CO_2 reduction. Ramanathan and Murali [126] investigated the photocatalytic degradation behaviour of SnO_2 NPs for MB, MO, RhB, and textile dyes under UV-Visible light radiation. The pseudo-first-order rate constants of four dyes were calculated from observation and measurement. The removal efficiencies of various dyes were investigated, and it was found that MB had a larger efficiency (93%) than all other dyes. The maximum degradation was brought on within 90 min by 30 mg/L tin oxide at pH 11. Oluwole and Olatunji [127] used a SnO_2/g-C_3N_4 nanocomposite to investigate the photodegradation of tetracycline. In comparison to g-C_3N_4 and SnO_2, which had degradation efficiencies of 40.9 % and 51.3 %, the degradation efficiencies of tetracycline by 1 wt.%, 2 wt.%, 3 wt.%, and 5 wt.% of SnO_2/g-C_3N_4 photocatalyst were 81.5%, 90.5%, 95.9%, and 92.1%. Ag doped SnO_2 for the photocatalytic degradation of MB dye was reported by Shittu et al. [128]. In comparison to undoped SnO_2, the photocatalytic activity findings show that 1wt% of Ag/SnO_2 has a superior photocatalytic performance of 97.63%.

The use of SnO_2/r-GO-based nanocomposite as electrode material for SCs was investigated by Joshi et al. [12]. At a current of 1 A/g, the maximum specific capacitance of the nanocomposite was observed to be 267.8 F/g. After 5000 GCD cycles, the SnO_2/r-GO electrode material was also found to be highly stable. Effectiveness of quantum dot-based nanocomposite materials in electrochemical energy storage systems was reported by Babu et al. [129]. In this work, nanocomposites of SnO_2 quantum dots and Au nanoparticles were used as an electrode material. The electrode material showed good specific capacity of 87 mAh/g at 1 A/g. After 5000 GCD cycles, the electrode's columbic efficiency was determined to be 98%. Fe_2O_3/SnO_2 nanocomposite was employed as an electrode material for SCs by Safari et al. [91]. In a three-electrode system, the Fe_2O_3/SnO_2 electrode exhibited excellent cycling stability, with 92.8 % capacitance retention at a high current density of 10 A/g after 3000 cycles. The specific capacitance was found to be 562.3 F/g at a current density of 1 A/g. Li et al. [130] investigated composites made of Sn/SnO_2 and graphene/carbon nanofibers for high performance SCs. The electrode material exhibits a high specific capacitance of 1349 F/g at 1 A/g and a remarkable rate capability of 88.9% retention at 20 A/g.

Populus ciliate leaf extract was used by Din et al. [112] for the green synthesis of SnO_2 NPs. *S. pyogene*, *S. aureus*, *K. pneumoniae* and *E. coli* used to observe the antibacterial properties of the SnO_2 NPs using the agar well diffusion technique. *S. pyogene* and *S. aureus* are more resistant to SnO_2 NPs than *K. pneumoniae* and *E. coli*. Preethi et al. [118] tested the antibacterial behaviour of Fe/SnO_2 against *E. coli* using the colony count technique, and they found that the inhibition rates were 49, 65, 70, and 78% for pure, 0.01, 0.03, and 0.05 M, respectively. Anuja et al. [121] studied the antibacterial activity of Al-Bi co-doped/SnO_2 and found the zone of inhibition in the range of 20 to 36 mm against *S. aureus*, 25 to 34 against *B. cereus* and 30 to 41 against *E. Coli*. Parameswari and Sakthivelu [131] studied the green synthesis of Co/Fe/SnO_2 using leaf extract of *Psidium guajava*. The antibacterial activity of the Co/Fe/SnO_2 was found to be higher than that of the conventional antibiotic amoxicillin. Additionally, Co/Fe/SnO_2 were found to be harmful to L929 cells following a 24-hour incubation period when utilised against breast cancer (MDA-MB-231) cell lines.

7. Conclusions:

The applications of nanomaterials in different fields of science and technology have proven how nanotechnology can overcome the divide among physical and biological sciences. Nanomaterials are made up of nanoparticles, which are formed at the atomic or molecular level. The development of innovative, environmentally friendly, and functional nanoproducts is the main challenge in nanomaterials and technologies. Tin oxide nanoparticles (SnO_2 NPs) have drawn considerable attention recently due to their fascinating properties. Water purification, batteries, SCs, antibacterial, and antioxidant, and other fields of study have all demonstrated the efficacy of SnO_2 NPs. SnO_2-based nanomaterials found numerous possibilities after the incorporation of components with different chemical compositions. We have addressed the basic characteristics, widespread uses, and in particular the photocatalytic degradation of organic pollutants, energy storage, and antibacterial activities in this article. SnO_2 NPs and their composites have been found to be efficient photocatalysts, electrode materials, and antibacterial agents based on the study's overall findings.

Supplementary Materials: Not applicable.

Author Contributions: Conceptualization, Naveen Chandra Joshi; software, Naveen Chandra Joshi, Niraj Kumar; data curation, Sanjay Upadhyay; writing—Naveen Chandra Joshi; writing—review and editing, Naveen Chandra Joshi, S Chetana.

Funding: N/A.

Institutional Review Board Statement: Not applicable.

Informed Consent Statement: Not applicable.

Data Availability Statement: The data can be obtained from the authors on request.

Acknowledgments: We are thankful to the Division of Research and Innovation for their encouragement and providing seed funding for conducting experiments.

Conflicts of Interest: The authors declare no conflict of interest.

References

1. Stankic, S.; Suman, S.; Haque, F.; Vidic, J. Pure and multi metal oxide nanoparticles: synthesis, antibacterial and cytotoxic properties. *J. Nanobiotechnol*. **2016**, 14, 1-20.
2. Rastogi, A.; Zivcak, M.; Sytar, O.; Kalaji, H.M.; He, X.; Mbarki, S.; Brestic, M. Impact of metal and metal oxide nanoparticles on plant: A critical review. *Frontiers in Chem*. **2017**. https://doi.org/10.3389/fchem.2017.00078.
3. Nikolova, M.P.; Chavali M.S. Metal oxide nanoparticles as biomedical materials. *Biomimetics (Basel)* **2020**, 5, 27.
4. Baig, N.; Kammakakam, I.; Falath, W. Nanomaterials: a review of synthesis methods, properties, recent progress, and challenges. *Mater. Advan*. **2021**. https://doi.org/10.1039/d0ma00807a.
5. Ramola, B.; Joshi, N.C.; Ramola, M.; Chhabra, J.; Singh, A. Green Synthesis, characterisations and antimicrobial activities of CaO nanoparticles. *Oriental J. Chem*. **2019**, 35, 1154-1157.
6. Joshi, N.C.; Prakash, Y. Leaves extract-based biogenic synthesis of cupric oxide nanoparticles, characterizations, and antimicrobial activity. *Asian J. Pharm. Clin. Res*. **2019**, 12, 288-291.
7. Gebreslassie, Y.T.; Gebretnsae, H.G. Green and cost-effective synthesis of tin oxide nanoparticles: A review on the synthesis methodologies, mechanism of formation, and their potential applications. *Nanoscale Res. Lett*. **2021**. https://doi.org/10.1186/s11671-021-03555-6.
8. Zhao, Q.; Ma, L.; Zhang, Q.; Wang, C.; Xu, X. SnO2-based nanomaterials: synthesis and application in lithium-ion batteries and supercapacitors. *J. Nanomater*. **2015**. https://doi.org/10.1155/2015/850147.
9. Dheyab, M.A.; Aziz, A.A.; Jameel, M.S.; Oladzadabbasabadi, N. Recent advances in synthesis, modification, and potential application of tin oxide nanoparticles. *Surfac. Interfac*. **2021**. https://doi.org/10.1016/j.surfin.2021.101677.
10. Karmaoui, M.; Jorge, A.B.; McMillan, P.F.; Aliev, A.E.; Pullar, R.C.; Labrincha, J.A.; Tobaldi, D.M. One-Step Synthesis, structure, and band gap properties of SnO_2 nanoparticles made by a low temperature nonaqueous sol–gel technique. *ACS Omega* **2018**, 10, 13227-13238.
11. Sun, C.; Yang, J.; Xu, M.; Cui, Y.; Ren, W.; Zhang, J.; Zhao, H.; Liang, B. Recent intensification strategies of SnO_2-based photocatalysts: A review. *Chemical Engin. J*. **2022**. https://doi.org/10.1016/j.cej.2021.131564.

12. Joshi, N.C.; Rawat, B.S.; Bisht, H.; Gajraj, V.; Kumar, N.; Chetana, S.; Gururani, P. Synthesis and supercapacitive behaviour of SnO_2/r-GO nanocomposite. *Synthetic Metals* **2022**. https://doi.org/10.1016/j.synthmet.2022.117132.
13. Kim, S.P.; Choi, M.Y.; Choi, H.C. Photocatalytic activity of SnO_2 nanoparticles in methylene blue degradation. *Mater. Rese. Bulletin* **2016**, 74, 85-89.
14. Amininezhad, S.M.; Rezvani, A.; Amouheidari, M.; Amininejad, S.M.; Rakhshani, S. The antibacterial activity of SnO_2 nanoparticles against Escherichia coli and Staphylococcus aureus. *Zahedan J. Res. Medical Sci*. **2015**, 17, 9.
15. Paramarta, V.; Taufik, A.; Munisa, L.; Saleh, R. Sono-and photocatalytic activities of SnO_2 nanoparticles for degradation of cationic and anionic dyes. *In AIP Conference Proceedings* **2017**, 1788, 030125.
16. Choudhary, A,K.; Gupta, A.; Kumar, S.; Kumar, P.; Singh, R.P.; Singh, P.; Kumar, V. Synthesis, antimicrobial activity, and photocatalytic performance of Ce doped SnO_2 nanoparticles. *Frontiers Nanotechn*. **2020**, 2, 595352.
17. Jarzebski, Z.M. Physical properties of SnO_2 materials, J. Electrochemi. Soci. 123 (1976) 199.
18. A.A. Baig, R. Vadamalar, K. Gnanamoorthi, K. Mohanraj, P. Jayanthi. Structural and morphological properties of tin oxide (SnO_2) nanoparticles by microwave irradiation method. *I.J.S.R.R.* **2018**, 7, 476-486.
19. Sen, M. Nanocomposite Materials. In (Ed.), Nanotechnology and the Environment. *IntechOpen*. **2020**. https://doi.org/10.5772/intechopen.93047.
20. Yadav, S.; Rani, N.; Saini, K. A review on transition metal oxides based nanocomposites, their synthesis techniques, different morphologies and potential applications. *In IOP Conference Series: Mater. Sci. Engin*. **2022**, 1225, 012004.
21. Sultana, S.; Khan, M.Z.; Umar, K.; Ahmed, A.S.; Shahadat, M. SnO_2–SrO based nanocomposites and their photocatalytic activity for the treatment of organic pollutants. *J. Molec. Struc*. **2015**, 1098, 393-399.
22. Tyagi, P.; Sharma, A.; Tomar, M.; Gupta, V. A comparative study of RGO-SnO_2 and MWCNT-SnO_2 nanocomposites based SO_2 gas sensors. *Sensors and Actuators B: Chem*. **2017**, 248, 980-986.
23. Liang, J.; Zhang, Y.; Wang, Z.; Zhang, Y.; Wang, K.; Chen, J.; Guo, X.; Wu, J.; Xu, Y.; Zhu, J.; Zhao, H.; Liang, J.; Wang, H. Binder-free 3D SnO_2-based nanocomposites anode with high areal capacity for advanced sodium-ion batteries. *Mater. Chem. Front*. **2022**, 6, 2803.
24. Tripathi, R.M.; Chung, S.J. Eco-friendly synthesis of SnO_2-Cu nanocomposites and evaluation of their peroxidase mimetic activity. *Nanomaterials* **2021**, 11, 1798.
25. Dontsova, T.A.; Kutuzova, A.S.; Bila, K.O.; Kyrii, S.O.; Kosogina, I.V.; Nechyporuk. D.O. Enhanced photocatalytic activity of TiO_2/SnO_2 binary nanocomposites. *J. Nanomater*. **2020**. https://doi.org/10.1155/2020/8349480.
26. Yin, X.T.; Li, J.; Wang, Q.; Dastan, D.; Shi, Z.C.; Alharbi, N.; Garmestani, H.; Tan, X.; Liu, Y.; Ma, X. Opposite sensing response of heterojunction gas sensors based on SnO_2–Cr_2O_3 nanocomposites to H_2 against CO and its selectivity mechanism. *Langmuir* **2021**, 37, 13548-13558.
27. Arvani, M.; Mohammad, H.A.; Khodadadi, A.A.; Mortazavi, Y. Graphene oxide/SnO_2 nanocomposite as sensing material for breathalyzers: selective detection of ethanol in the presence of automotive CO and hydrocarbons emissions. *Scientia Iranica* **2017**, 24, 3033-3040.
28. Sharma, A.; Ahmed, A.; Singh, A.; Oruganti, S.K.; Khosla, A.; Arya, S. Recent advances in tin oxide nanomaterials as electrochemical/chemiresistive sensors. *J. Electrochem. Soci*. **2021**, 168, 027505.
29. Kondawar, S.B.; Agrawal, S.P.; Nimkar, S.H.; Sharma, H.J.; Patil, P.T. Conductive polyaniline-tin oxide nanocomposites for ammonia sensor. *Advan. Mater. Lett*. 2012, 3, 393-398.
30. Pandiyan, R.; Mahalingam, S.; Ahn, Y.H. Antibacterial and photocatalytic activity of hydrothermally synthesized SnO_2 doped GO and CNT under visible light irradiation. *J. Photochem. Photobio. B: Biolo*. **2019**, 191, 18-25.
31. Saeed, M.; Muneer, M.; Haq, A.; Akram, V. Photocatalysis: an effective tool for photodegradation of dyes—a review. *Environ. Sci. Pollut. Res*. **2022**, 29, 293-311.
32. Joshi, N.C.; Gururani, P.; Gairola, S.P. Metal oxide nanoparticles and their nanocomposite-based materials as photocatalysts in the degradation of dyes. *Biointerface Res. Appl. Chem*. **2022**, 12, 6557.
33. Nazri, M.K.H.; Sapawe, N. A short review on photocatalytic toward dye degradation. *Mater. Today: Proceed*. **2020**, 31, A42-A47.
34. Joshi, N.C.; Gururani, P. Advances of graphene oxide-based nanocomposite materials in the treatment of wastewater containing heavy metal ions and dyes. *Current Rese. Green Sustain. Chem*. **2022**. https://doi.org/10.1016/j.crgsc.2022.100306.
35. Khan, M.M.; Adil, S.F.; Al-Mayouf, A. Metal oxides as photocatalysts. *J. Saudi chem. Soci*. **2015**, 19, 462-464.
36. Chiu, Y.H.; Chang, T.F.M.; Chen, C.Y.; Sone, M.; Hsu, Y.J. Mechanistic insights into photodegradation of organic dyes using heterostructure photocatalysts. *Catalysts* **2019**, 9, 430.

37. Kumar, A.; Pandey, G. A review on the factors affecting the photocatalytic degradation of hazardous materials. *Material Sci. Eng. Int. J.* **2017**, 1, 106-114. https://doi.org/10.15406/mseij.2017.01.00018
38. Gnanaprakasam, A.; Sivakumar, V.M.; Thirumarimurugan, M. Influencing parameters in the photocatalytic degradation of organic effluent via nanometal oxide catalyst: A review. *Indian J. Mater. Sci*. **2015**. https://doi.org/10.1155/2015/601827.
39. Reza, K.M.; Kurny, A.; Gulshan, F. Parameters affecting the photocatalytic degradation of dyes using TiO2: a review. *Appl. Water Sci*. **2017**, 7, 1569-1578. https://doi.org/10.1007/s13201-015-0367-y
40. Abbas, M. Factors influencing the adsorption and photocatalysis of direct red 80 in the presence of a TiO_2: Equilibrium and kinetics modelling. *J. Chem. Res*. **2021**, 45, 694.
41. Joshi, N.C.; Gaur, A.; Singh, A. Synthesis, characterisations, adsorptive performances and photo-catalytic activity of Fe_3O_4-SiO_2 based nanosorbent (Fe_3O_4-SiO_2 BN). *J. Inorganic Organomet. Polym. Mater*. **2020**, 30, 4416-4425.
42. Kaur, M.; Prasher, D.; Sharma, R. Recent developments on I and II Series transition elements doped SnO_2 nanoparticles and its applications for water remediation process: A review. *J. Water Environ. Nanotech*. **2022**, 7, 194-217.
43. Low, J.; Yu, J.; Jaroniec, M.; Wageh, S.; Al-Ghamdi, A.A. Heterojunction Photocatalysts. *Advanced Mater*. **2017**. https://doi.org/10.1002/adma.201601694.
44. Thongam, D.D.; Chaturvedi, H. Advances in nanomaterials for heterogeneous photocatalysis. *Nano Express* **2021**, 2, 012005.
45. Xing, L.; Dong, Y.; Wu, X. SnO_2 nanoparticle photocatalysts for enhanced photocatalytic activities. *Materials Res. Expr*. **2018**, 5, 085026.
46. Yuan, H.; Xu, J. Preparation, characterization and photocatalytic activity of nanometer SnO_2. *Intern. J. Chem. Engin. Appl*. **2020**, 1(3), 241-246.
47. He, Z.; Zhou, J. Synthesis, characterization, and activity of tin oxide nanoparticles: influence of solvothermal time on photocatalytic degradation of rhodamine B. *Mod. Res. Catal*. **2013**, 2, 13-18.
48. Tammina, S.K.; Mandal, B.K.; Kadiyala, N.K. Photocatalytic degradation of methylene blue dye by nonconventional synthesized SnO_2 nanoparticles. *Environ. Nanotech. Monit. Manag*. **2018**, 10, 339-350.
49. Pouretedal, H.R.; Shafeie, A.; Keshavarz, M.H. Preparation, characterization and catalytic activity of tin dioxide and zero-valent tin nanoparticles. *J. Korean Chem. Soc*. **2012**, 56, 484-490.
50. Suresh, K.C.; Surendhiran, S.; Kumar, P.M.; Kumar, E.R.; Khadar, Y.A.S.; Balamurugan, A. Green synthesis of SnO_2 nanoparticles using Delonix elata leaf extract: Evaluation of its structural, optical, morphological and photocatalytic properties. *SN Appl. Sci*. **2020**. https://doi.org/10.1007/s42452-020-03534-z.
51. Karthik, K.; Revathi, V.; Tatarchuk, T. Microwave-assisted green synthesis of SnO_2 nanoparticles and their optical and photocatalytic properties. *Mole. Crys. Liq. Crys*. **2018**, 671, 17-23.
52. Wicaksono, W.P.; Sahroni, I.; Saba, A.K.; Rahman, R.; Fatimah, I. Biofabricated SnO_2 nanoparticles using Red Spinach (Amaranthus tricolor L.) extract and the study on photocatalytic and electrochemical sensing activity. *Mater. Res. Expr*. **2020**, 7, 075009.
53. Singh, J.; Kaur, H.; Kukkar, D.; Mukamia, V.K.; Kumar, S.; Rawat, M. Green synthesis of SnO_2 NPs for solar light induced photocatalytic applications. *Mater. Res. Express* **2019**, 6, 115007.
54. Viet. P.V.; Thi, C.M.; Hieu, L.V. The High Photocatalytic Activity of SnO_2 Nanoparticles Synthesized by Hydrothermal Method. *J. Nanomate*. **2016**. https://doi.org/10.1155/2016/4231046.
55. Fatimah, I.; Purwiandono, G.; Hidayat, H.; Sagadevan, S.; Ghazali, S.A.I.S.M.; Oh, W.C.; Doong, R.A. Flower-like SnO_2 nanoparticle biofabrication using pometia pinnata leaf extract and study on its photocatalytic and antibacterial activities. *Nanomater*. **2021**, 11, 3012.
56. Sujatmiko, F.; Sahroni, I.; Fadillah, G.; Fatimah, I. Visible light-responsive photocatalyst of SnO_2/rGO prepared using Pometia pinnata leaf extract. *Open Chem*. **2021**, 19, 174-183.
57. Sayadi, M.H.; Homaeigohar, S.; Rezaei, A.; Shekari, H. Bi/SnO_2/TiO_2-graphene nanocomposite photocatalyst for solar visible light–induced photodegradation of pentachlorophenol. *Environ. Sci. Pollut. Res*. **2021**, 28, 15236-15274.
58. Yao, S.; Zhou, S.; Wang, J.; Li, W.; Li, Z. Optimizing the synthesis of SnO_2/TiO_2/RGO nanocomposites with excellent visible light photocatalytic and antibacterial activities. *Photochem. Photobiol. Sci*. **2019**, 18, 2989-2999.
59. Długosz, O.; Banach, M. ZnO–SnO_2–Sn nanocomposite as photocatalyst in ultraviolet and visible light. *Appl. Nanosci*. **2021**, 11, 1707-1719.
60. Kaur, D.; Bagga, V.; Behera, N.; Thakral, B.; Asija, A.; Kaur, J.; Kaur, S. SnSe/SnO_2 nanocomposites: novel material for photocatalytic degradation of industrial waste dyes. *Adv. Compos. Hybrid Mater*. **2019**, 2, 763-776.

61. Vinosel, V.M.; Anand, S.; Janifer, M.A.; Pauline, S.; Dhanavel, S.; Praveena, P.; Stephen, A. Enhanced photocatalytic activity of Fe_3O_4/SnO_2 magnetic nanocomposite for the degradation of organic dye. *J. Mater. Sci: Mater. Electron*. **2019**, 30, 9663-9677.
62. Roy, A.; Arbuj, S.; Waghadkar, Y.; Shinde, M.; Umarji, G.; Rane, S.; Patil, K.; Gosavi, S.; Chauhan, V. Concurrent synthesis of SnO/SnO_2 nanocomposites and their enhanced photocatalytic activity. *J. Solid State Electrochem*. **2017**, 21, 9-17.
63. Begum, S.; Mishra, S.R.; Ahmaruzzaman, M. Fabrication of $ZnO–SnO_2$ nanocomposite and its photocatalytic activity for enhanced degradation of Biebrich scarlet. *Environ. Sci. Pollut. Res*. **2022**. https://doi.org/10.1007/s11356-022-21851-1.
64. Suganya, M.; Balu, A.R.; Prabha, D.; Anitha, S.; Balamurgan, S.; Srivind, J. PbS SnO_2 nanocomposite with enhanced magnetic, photocatalytic and antifungal properties. *J. Mater. Sci.: Mater. Electron*. **2018**, 29, 1065.
65. Singh, P.; Kaur, G.; Singh, K.; Singh, B.; Kaur, M.; Kaur, M.; Krishnan, U.; Kumar, M.; Bala, R.; Kumar, A. Specially designed B_4C/SnO_2 nanocomposite for photocatalysis: traditional ceramic with unique properties. *Appl. Nanosci*. **2018**. https://doi.org/10.1007/s13204-018-0662-7.
66. Kumar, M.R.; Murugadoss, G.; Pirogov, A.N.; Thangamuthu, R. A facile one step synthesis of SnO_2/CuO and CuO/SnO_2 nanocomposites: photocatalytic application. *J. Mater. Sci.: Mater. Electron*. **2018**, 29, 13508-13515.
67. Babu, B.; Harish, V.V.N.; Shim, J.; Reddy, C.V. Solution combustion synthesis of SnO_2–NiO p–n heterojunction nanocomposite for photocatalytic application. *J. Mater. Sci.: Mater. Electron*. **2018**, 29, 16988-16996.
68. Huang, Q.; Zhao, Q.; Yang, C.; Jiang, T. Facile synthesis of mesoporous graphitic carbon nitride/SnO_2 nanocomposite photocatalysts for the enhanced photodegradation of Rhodamine B. *Reac. Kinet. Mech. Cat*. **2020**, 129, 535-550.
69. Abdel Maksoud, M.I.A.; Fahim, R.A.; Shalan, A.E.; Alkodous, M.; Olojede, S.O.; Osman, A.I.; Farrell, C.; Almuhtaseb, A.; Awed, A.S.; Ashour, A.H.; Rooney, D.W. Advanced materials and technologies for supercapacitors used in energy conversion and storage: a review. *Environ. Chem. Lett*. **2021**, 19, 375-439.
70. Castro-Gutiérrez, J.; Celzard, A.; Fierro, V. Energy storage in supercapacitors: Focus on tannin-derived carbon electrodes. *Front. Mater*. **2020**. https://doi.org/10.3389/fmats.2020.00217.
71. Jimena, G.; Alain, C.; Vanessa, F. Energy storage in supercapacitors: Focus on tannin-derived carbon electrodes. *Front. Mater*. **2020**. https://doi.org/10.3389/fmats.2020.00217.
72. Gautham, P.G.; Shetty, N.; Thakur, S.; Rakshita, Bommegowda, K.B. Supercapacitor technology and its applications: a review. *IOP Conf Series Materials Science and Engineering* **2019**, 561, 012105.
73. Abdah, M.A.A.M.; Azman, N.H.M.; Kulandaivalu, S.; Sulaiman, Y. Review of the use of transition-metal-oxide and conducting polymer-based fibres for high-performance supercapacitors. *Mater. Desig*. **2020**, 186, 108199.
74. Rashid, M.H. Front Matter, Power Electronics Handbook (Third Edition), Elsevier *Butterworth-Heinemann* **2011**. https://doi.org/10.1016/B978-0-12-382036-5.00053-7.
75. González-García, P. Activated carbon from lignocellulosics precursors: A review of the synthesis methods, characterization techniques and applications. *Renew. Sust. Energy Rev*. **2018**, 82, 1393-1414.
76. Xie, J.; Yang, P..; Wang, Y.; Qi, T.; Lei, Y.; Li, C.M. Puzzles and confusions in supercapacitor and battery: theory and solutions. *J. Power Sources* **2018**, 401, 213-223.
77. Prasankumar, T.; Jose, J.; Jose, S.; Balakrishnan, S.P. Pseudocapacitors In D. Tashima, & A. K. Samantara (Eds.), Supercapacitors for the Next Generation. *IntechOpen* **2021**. https://doi.org/10.5772/intechopen.98600.
78. Zhou, L.; Li, C.; Liu, X.; Zhu, Y.; Wu, Y.; Ree, T. Metal oxides in supercapacitors. *Metal Oxides in Energy Techn*. **2018**. https://doi.org/10.1016/B978-0-12-811167-3.00007-9.
79. Fleischmann, S.; Mitchell, J.B.; Wang, R.; Zhan, C.; Jiang, D.; Presser, V.; Augustyn, V. Pseudocapacitance: From fundamental understanding to high power energy storage materials. *Chemical Reviews* **2020**, 120, 6738-6782.
80. Muzaffar, A.; Ahamed, M.B.; Deshmukh, K.; Thirumalai, J. A review on recent advances in hybrid supercapacitors: Design, fabrication and applications. *Renew. Sustain. Energy Reviews* **2019**, 101, 123-145.
81. Manikandan, K.; Dhanuskodi, S.; Maheswari, N.; Muralidharan G. SnO_2 nanoparticles for supercapacitor application. *AIP Conference Proceedings* **2016**, 1731, 050048.
82. Velmurugan, V.; Srinivasarao, U.; Ramachandran, R.; Saranya, M.; Grace, A.N. Synthesis of tin oxide/graphene (SnO_2/G) nanocomposite and its electrochemical properties for supercapacitor applications. *Mater. Rese. Bulle*. **2016**, 84, 145-151.
83. Wang, W.; Hao, Q.; Lei, W.; Xia, X.; Wang, X. Graphene/SnO_2/polypyrrole ternary nanocomposites as supercapacitor electrode materials. *RSC Advan*. **2012**, 2, 10268.

84. Ramesh, S.; Yadav, H.M.; Lee, Y.J.; Hong, G.W.; Kathalingam, A.; Sivasamy, A.; Kim, H.S.; Kim, J.H. Porous materials of nitrogen doped graphene oxide@SnO_2 electrode for capable supercapacitor application. *Scien. Rep*. **2019**, 9, 1.
85. Samuel, E.; Kim, T.G.; Park, C.W.; Joshi, B.; Swihart, M.T.; Yoon, S.S. Supersonically sprayed Zn_2SnO_4/SnO_2/CNT nanocomposites for high-performance supercapacitor electrodes. *ACS Sustain. Chem. Engin*. **2019**, 7, 14031-14040.
86. Feng, W.; Liu, G.; Wang, P.; Zhou, J.; Gu, L.; Chen, L.; Li, X.; Dan, Y.; Cheng, X. Template synthesis of a hetero-structured MnO_2@ SnO_2 hollow sphere composite for high asymmetric supercapacitor performance. *ACS App. Energy Mater*. **2020**, 3, 7284-7293.
87. Zhang, Y.; Liu, M.; Sun, S.; Yang, L. The preparation and characterization of SnO_2/rGO nanocomposites electrode materials for supercapacitor. Compos. Advan. Mate. **2020**. https://doi.org/10.1177/2633366X20909839.
88. Liu, Y.; Jiao, Y.; Yin, B.; Zhang, S.; Qu, F.; Wu, X. Enhanced electrochemical performance of hybrid SnO_2@ MOx (M= Ni, Co, Mn) core–shell nanostructures grown on flexible carbon fibers as the supercapacitor electrode materials. *J. Mater. Chemi*. **2015**, A 3, 3676.
89. Chuai, M.; Chen, X.; Zhang, K.; Zhang, J.; Zhang, M. CuO–SnO_2 reverse cubic heterojunctions as high-performance supercapacitor electrodes. *J. Mater. Chem*. **2019**, A 7, 1160.
90. Varshney, B.; Siddiqui, M.J.; Anwer, A.H.; Khan, M.Z.; Ahmed, F.; Aljaafari, A.; Hammud, H.H.; Azam, A. Synthesis of mesoporous SnO_2/NiO nanocomposite using modified sol–gel method and its electrochemical performance as electrode material for supercapacitors. *Scien. Rep*. **2020**, 10, 11032.
91. Safari, M.; Mazloom, J.; Boustani, J.; Monemdjou, A. Hierarchical Fe_2O_3 hexagonal nanoplatelets anchored on SnO_2 nanofibers for high-performance asymmetric supercapacitor device. *Sci. Rep*. **2022**, 12, 14919.
92. Lin, L.; Chen, S.; Deng, T.; Zeng, W. Oxygen-deficient stannic oxide/graphene for ultrahighperformance supercapacitors and gas sensors. *Nanomater*. **2021**. https://doi.org/10.3390/nano11020372.
93. Huang, M.; Zhao, X.L.; Li, F.; Li, W.; Zhang, B.; Zhang, Y.X. Synthesis of Co_3O_4/SnO_2@ MnO_2 core–shell nanostructures for high-performance supercapacitors. *J. Mater. Chem. A* **2015**, 3, 12852.
94. Yan, J.; Khoo, E.; Sumboja, A.; Lee, P.S. Facile coating of manganese oxide on tin oxide nanowires with high-performance capacitive behavior. *ACS Nano*. **2010**, 27, 4247-4255.
95. Ng, K.C.; Zhang, S.; Chen, C.Z. An asymmetrical supercapacitor based on CNTs/SnO_2 and CNTs/MnO_2 nanocomposites working at 1.7 v in aqueous electrolyte. *ECS Trans*. **2008**. https://doi.org/10.1149/1.2985638.
96. Dai, Y.M.; Tang, S.C.; Peng, J.Q.; Chen, H.Y.; Ba, Z.X.; Ma, Y.J.; Meng, X.K. MnO_2@SnO_2 core–shell heterostructured nanorods for supercapacitors. *Mater. Lett*. **2014**, 130, 107-110.
97. Albalghiti, E.; Stabryla, L.M.; Gilbertson, L.M.; Zimmerman, J.B. Towards resolution of antibacterial mechanisms in metal and metal oxide nanomaterials: a meta-analysis of the influence of study design on mechanistic conclusions. *Environ. Sci.: Nano* **2021**, 8, 37-66.
98. Slavin, Y.N.; Asnis, J.; Häfeli, U.O.; Bach, H. Metal nanoparticles: understanding the mechanisms behind antibacterial activity. *J. Nanobiotechnol*. **2017**. https://doi.org/10.1186/s12951-017-0308-z.
99. John, N.; Somaraj, M.; Tharayil, N.J. Synthesis, characterization and anti–bacterial activities of SnO_2 nanoparticles using biological molecule. *IOP Conference Series: Materials Sci. Engin*. **2018**, 360, 012007.
100. Vega-Jiménez, L.; Alejandro, A.R.; Vázquez-Olmos, E.; Acosta-Gío, M.A.; Álvarez-Pérez. In vitro antimicrobial activity evaluation of metal oxide nanoparticles. *Nanoemulsions Prop. Fabr. Appl*. **2019**. https://doi.org/10.5772/intechopen.84369.
101. Dizaj, S.M.; Lotfipour, F.; Barzegar-Jalali, M.; Zarrintan, M.H.; Adibkia, K. Antimicrobial activity of the metals and metal oxide nanoparticles. *Mater. Sci. Engin.: C* **2014**, 44, 278-284.
102. Choudhary, A.K.; Gupta, A.; Kumar, S.; Kumar, P.; Singh, R.P.; Singh, P.; Kumar, V. Synthesis, antimicrobial activity, and photocatalytic performance of Ce doped SnO_2 nanoparticles. *Front. Nanotechn*. **2020**, 2 , 595352.
103. Yemmireddy, V.K.; Hung, Y.C. Using photocatalyst metal oxides as antimicrobial surface coatings to ensure food safety-opportunities and challenges. *Compr. Rev. Food Sci. Food Saf*. **2017**, 16, 617-631.
104. Abebe, B.; Zereffa, E.A.; Tadesse, A.; Murthy, H.C.A. A Review on enhancing the antibacterial activity of ZnO: Mechanisms and microscopic investigation. *Nanoscale Res. Lett*. **2020**. https://doi.org/10.1186/s11671-020-03418-6.
105. Wang, L.; Hu, C.; Shao. L. The antimicrobial activity of nanoparticles: present situation and prospects for the future. *Intern. J. Nanomed*. **2017**, 12, 1227.
106. Apsana, G.; George, P.P. A green approach to phyto-mediated synthesis of SnO_2 nanoparticles using ocimum sanctum leaf extract and their antibacterial properties. *Materials Focus* **2018**, 7, 790-797.

107. Ayeshamariam, A.; Begam, M.; Jayachandran, M.; Kumar, G.P.; Bououdina, M. Green synthesis of nanostructured materials for antibacterial and antifungal activities. *Int. J. Bioassays* **2013**, 2, 304-311.
108. Khanom, R.; Parveen, S.; Hasan, M. Antimicrobial activity of SnO_2 nanoparticles against Escherichia coli and Staphylococcus aureus and conventional antibiotics. *American Acad. Sci. Res. J. Eng. Tech. Sci*. **2018**, 46, 111-121.
109. Kamaraj, P.; Vennila, R.; Arthanareeswari, M.; Devikala, S. Biological activities of tin oxide nanoparticles synthesized using plant extract. *World J. Pharm. Pharmaceut. Sci*. **2014**, 3, 382.
110. Gowri, S.; Gandhi, R.R.; Sundrarajan, M. Green synthesis of tin oxide nanoparticles by aloe vera: structural, optical and antibacterial properties. *J. Nanoelectron. Optoelectron*. **2013**, 8, 240.
111. Fatimah, I.; Purwiandono, G.; Hidayat, H.; Sagadevan, S.; Ghazali, S.A.I.S.M.; Oh, W.C.; Doong, R.A. Flower-like SnO_2 nanoparticle biofabrication using pometia pinnata leaf extract and study on its photocatalytic and antibacterial activities. *Nanomater*. **2021**, 11, 3012.
112. Din, S.U.; Kiani, S.H.; Haq, S.; Ahmad, P.; Khandaker, M.U.; Faruque, M.R.I.; Idris, A.M.; Sayyed, M.I. Biosynthesized tin oxide nanoparticles: structural, optical, and biological studies. *Crystals* **2022**. https://doi.org/10.3390/ cryst12050614.
113. Obeizia, Z.; Benbouzidb, H.; Bouarroudjc, T.; Benzaidd, C.; Djahoudie, A. Synthesis, characterization of (Ag-SnO_2) nanoparticles and investigation of its antibacterial and anti-biofilm activities. *J. New Technol. Mater*. **2021**, 10, 10-17.
114. Sathishkumar, M.; Geethalakshmi, S. Enhanced photocatalytic and antibacterial activity of Cu:SnO_2 nanoparticles synthesized by microwave assisted method. *Materials Today: Proceed*. **2020**, 20, 54.
115. Omar, K.; Meena, B.I.; Muhammed, S.A. Study on the activity of ZnO-SnO_2 nanocomposite against bacteria and fungi. *Physicochem. Probl. Miner. Process*. 2016, 52, 754−766.
116. Qamar, M.A.; Shahid, S.; Khan, S.A.; Zaman, S.; Sarwar, M.N. Synthesis characterization, optical and antibacterial studies of Co-doped SnO_2 nanoparticles. *Dig. J. Nanomater. Biostruct*. **2017**, 12, 1127-1135.
117. Ali Baig, A.B.; Rathinam, V.; Palaninathan, J. Fabrication of Zr-doped SnO_2 nanoparticles with synergistic influence for improved visible-light photocatalytic action and antibacterial performance. *Appl. Water Sci*. **2020**. https://doi.org/10.1007/s13201-019-1119-1
118. Preethi, T.; Senthil, K.; Pachamuthu, M.P.; Balakrishnaraja, R.; Sundaravel, B.; Geetha, N.; Bellucci, V. Effect of Fe Doping on Photocatalytic Dye-Degradation and Antibacterial Activity of SnO_2 Nanoparticles. *Ads. Sci. Tech*. **2022**. https://doi.org/10.1155/2022/9334079.
119. Mostafa, A.M.; Mwafy, E.A. Effect of dual-beam laser radiation for synthetic SnO_2/Au nanoalloy for antibacterial activity. *J. Molec. Struc*. **2020**, 1222, 128913.
120. Podurets, A.; Khalidova, M.; Chistyakova, L.; Bobrysheva, N.; Osmolowsky, M.; Voznesenskiy, M.; Osmolovskaya, O. Experimental and computational study of Ni-doped SnO2 as a photocatalyst and antibacterial agent for water remediation: The way for a rational design. *J. Alloy. Comp*. **2022**, 926, 166950.
121. Anuja, E.; Pramothkumar, A.; Brindha, R.; Vetha Potheher, P.I. Pure and Al-Bi Co-doped SnO_2 nanoparticles as bacterial growth inhibitors. *Toxic. Environ. Chem*. **2022**. https://doi.org/10.1080/02772248.2022.2117361.
122. Xiao, L.; Liao, R.; Yang, S.; Qiu, Y.; Wang, M.; Zhang, Z.; Du, J.; Xie, Z. Facile fabrication of F-doped SnO_2 nanomaterials for improved photocatalytic activity. *Coatings* **2022**. https://doi.org/10.3390/ coatings12060795.
123. Nazim, V.S.; El-Sayed, G.M.; Amer, S.M.; Nadim, A.H. Functionalized SnO_2 nanoparticles with gallic acid via green chemical approach for enhanced photocatalytic degradation of citalopram: synthesis, characterization and application to pharmaceutical wastewater treatment. *Environ. Sci. Pollut. Res*. **2022**. https://doi.org/10.1007/s11356-022-22447-5.
124. Długosz, O.; Staroń, A.; Brzoza, P.; Banach, M. Synergistic effect of sorption and photocatalysis on the degree of dye removal in single and multicomponent systems on ZnO-SnO_2. *Environ. Sci. Pollut. Res*. **2022**. https://doi.org/10.1007/s11356-021-18044-7.
125. Gao, S.; Guan, H.; Wang, H.; Yang, X.; Yang, W.; Li, Q. Creation of $Sn_xNb_{1-x}O_2$ solid solution through heavy Nb-doping in SnO_2 to boost its photocatalytic CO_2 reduction to C2+ products under simulated solar illumination. *J. Adv. Ceram* **2022**, 11, 1404-1416.
126. Ramanathan, G.; Murali, K.R. Photocatalytic activity of SnO_2 nanoparticles. *J. Appl. Electrochem*. **2022**, 52, 849-859.
127. Oluwole, A.O.; Olatunji, O.S. Photocatalytic degradation of tetracycline in aqueous systems under visible light irridiation using needle-like SnO_2 nanoparticles anchored on exfoliated g-C_3N_4. *Environ. Sci. Europe* **2022**, 34, 1-14.

128. Shittu, H.A.; Adedokun, O.; Kareem, M.A.; Sivaprakash, P.; Bello, I.T.; Arumugam, S. Effect of low-doping concentration on silver-doped SnO_2 and its photocatalytic applications. *B.R.I.A.C.* **2023**. https://doi.org/10.33263/BRIAC132.165.
129. Babu, B.; Kim, J.; Yoo, K. Nanocomposite of SnO_2 quantum dots and Au nanoparticles as a battery-like supercapacitor electrode material. *Mater. Lett*. **2022**, 15, 309.
130. Li, Z.; Zhang, C.; Bu, J.; Zhang, L.; Cheng, L.; Wu, M. Constructing a novel carbon skeleton to anchor Sn/SnO_2 nanodots for flexible supercapacitor with excellent rate capability. *Carbon* **2022**, 194, 197.
131. Parameswari, P.; Sakthivelu, A. Microwave-assisted green process of cobalt ferrous codoped tin oxide nanoparticles: Antibacterial, anticancer, and toxicity performance. *BioNanoSci*. **2022**. https://doi.org/10.1007/s12668-022-01042-5.